Journal of Power Sources 188 (2009) 635–641

Contents lists available at ScienceDirect

Journal of Power Sources

journal homepage: www.elsevier.com/locate/jpowsour

Influences of different TiO_2 morphologies and solvents on the photovoltaic performance of dye-sensitized solar cells

Kun-Mu Lee[a], Vembu Suryanarayanan[b], Kuo-Chuan Ho[a,c,*]

[a] Institute of Polymer Science and Engineering, National Taiwan University, Taipei 10617, Taiwan
[b] Electro Organic Division, Central Electrochemical Research Institute, Karaikudi 630 006, Tamil Nadu, India
[c] Department of Chemical Engineering, National Taiwan University, Taipei 10617, Taiwan

ARTICLE INFO

Article history:
Received 8 June 2008
Received in revised form
21 November 2008
Accepted 1 December 2008
Available online 6 December 2008

Keywords:
Dye-sensitized solar cells
Electron lifetime
TiO_2 morphology
Donor number
Solvent effect

ABSTRACT

The effects of TiO_2 photoelectrode's surface morphology and different solvents on the photovoltaic performance of dye-sensitized solar cells (DSSCs) were studied. By successive coating of TiO_2 suspension, composed of low and high molecular weight poly(ethylene)glycol (PEG) as a binder, double layered TiO_2 photoelectrodes with four different structures were obtained. Among the DSSCs with different TiO_2 electrodes, DSSC with P2P1 electrode (P2 and P1 correspond to PEG molecular weights of 20,000 and 200,000, respectively) showed higher performance under identical film thickness at a constant irradiation of 100 mW cm^{-2}, which may be correlated with large pore size and high surface area of the corresponding TiO_2 electrode. This was confirmed by electrochemical impedance spectroscopy (EIS) analysis of the DSSC and the transient photovoltage measurement of electrons in the TiO_2 electrode. Among the different solvents investigated here, the DSSC containing acetonitrile showed high conversion efficiency and the order of performance of the DSSCs with different solvents were AN > MPN > PC > GBL > DMA > DMF > DMSO. Better correlation was observed between the donor number of solvents and photoelectrochemical parameters of the DSSCs containing different solvents rather than the measured viscosity and dielectric constant of solvents. The reasons for the low performance of the DSSCs containing DMA, DMSO and DMF, respectively, were due to the negative shift of TiO_2 conduction band and the desorption of dye molecules from the TiO_2 photoelectrode by those solvents.

1. Introduction

In 1991, the successful demonstration of dye-sensitized solar cell (DSSC) introduced a novel approach to traditional inorganic silicon solar cells [1–3]. In these devices, photon-to-electricity conversion is achieved by ultrafast electron injection from a photo-excited dye into the conduction band of TiO_2 and subsequently dye regeneration and the hole transportation to the counter electrode. In order to improve the performance of the DSSC further, extensive research has been performed on each constituents of the solar cell such as semiconductor nano-crystalline TiO_2 [4–8], molecular dye [9–12], supporting electrolyte [13–16] and counter electrode [17,18].

The influence of surface morphology of TiO_2 coating on the performance of DSSC was already investigated in our laboratory [19]. Shen and Toyoda had studied the optical absorption and electron transport properties of the TiO_2 particles having different pore diameters and proposed that the use of small TiO_2 particles and large pore size led to the good electron transport [20]. However, if the pore diameter is too large, the surface area of the TiO_2 material will decrease, resulting in the poor adsorption of the dye molecules. Obviously, the nano-sized TiO_2 particles offer high surface areas leading to the adsorption of more dye molecules and at the same time, the possibilities of charge recombination will be high in the above-mentioned system. It is the most important thing to mention here that for getting a high photocurrent, the surface area of the TiO_2 thin film must be large. Nevertheless, if the pore diameter of TiO_2 is too small, iodide/tri-iodide (I_3^-/I^-) redox couple cannot be able to diffuse into TiO_2 thin film. Hence, all the three parameters such as the particle size, surface area and the porosity of the TiO_2 film influence the efficiency of the DSSCs significantly.

The role of solvent-supporting electrolyte system is prominent in the operation of DSSCs [21–23]. Kebede and Lindquist [14], and Hara et al. [15] investigated the spectrophotometric properties of I^-/I_3^- based electrolytes in different solvents and postulated that various properties such as donor number, viscosity and dielectric constant had influenced strongly the photophysical properties of the DSSCs. In a recent work, photovoltaic properties of the DSSC containing mixture of solvents such as tetrahydrofuran and acetonitrile were also studied in detail [21].

* Corresponding author at: Department of Chemical Engineering, National Taiwan University, Taipei 10617, Taiwan. Tel.: +886 2 2366 0739; fax: +886 2 2362 3040.
E-mail address: kcho@ntu.edu.tw (K.-C. Ho).

0378-7753/$ – see front matter © 2008 Elsevier B.V. All rights reserved.
doi:10.1016/j.jpowsour.2008.12.002

Based on these above studies, the effects of the TiO_2 morphology and solvents on the performance of DSSC were investigated. We prepared two kinds of the TiO_2 pastes using poly(ethylene glycol) (PEG) as a binder with two different molecular weights, respectively. Four different kinds of nanostructure of the TiO_2 photoelectrodes were fabricated by using each TiO_2 paste, which followed a simple preparation method. The electron transfer in the TiO_2 films, internal resistances and the cell performances of the four different composite layers of the TiO_2 electrode surface were studied. Further, transient electron lifetime measurements were used to investigate the characteristics of different TiO_2 surface morphologies and optimized the TiO_2 electrode. The relationship between solvent properties and cell performances was also investigated.

2. Experimental

2.1. Materials

Anhydrous acetonitrile (AN), propylene carbonate (PC), methoxy propionitrile (MPN), γ-butyro lactone (GBL), N,N′-dimethylformamide (DMF), N,N′-dimethylacetamide (DMA), dimethylsulfoxide (DMSO) and tert-butanol were purchased from Merck and water molecules were removed by putting molecular sieves (4 Å) into the solvents. Anhydrous LiI, I_2, poly(ethylene glycol) (PEG) and 4-tert-butyl pyridine (TBP) were obtained from Merck and titanium (IV) isopropoxide (>98%) was purchased from Acros. The cis-di(thiocyanato)bis(2,2′-bipyridyl-4,4′-dicarboxylate)ruthenium(II) (N3) was the commercial product, which obtained from Solaronix (Aubonne, Switzerland).

2.2. Preparation of the TiO_2 pastes

The TiO_2 colloids were prepared by the method modified from Grätzel and co-workers [4]. Titanium (IV) isopropoxide (72 ml, 98%) was added to 430 ml of 0.1 M nitric acid solution with constant stirring and the colloidal solution was heated to 85–90 °C simultaneously for 8 h. The mixture was cooled down to room temperature and filtered. Then the filtrate was heated in an autoclave at 240 °C for 12 h in order to allow the TiO_2 particles to grow uniformly. The solution was concentrated to 13 wt% and two types of TiO_2 pastes namely P1 and P2 which were prepared by the addition of 30 wt% (with respect to TiO_2) of PEG with the corresponding molecular weights of 20,000 and 200,000, respectively, to the above solution in order to control the pore diameters and to prevent the film from cracking during drying.

2.3. Fabrication of double-layered TiO_2 electrodes and assembly of cells

Those two TiO_2 pastes (P1 and P2) were coated on a fluorine-doped tin oxide (FTO) glass plate using glass rod method [4,11] (The FTO sheet resistance is 15 $\Omega\,sq^{-1}$). Using these two types of pastes, four different kinds of film structures of the TiO_2 material were obtained by different coating procedures. For example, P1P1 and P2P2 represent the coating of P1 over P1 or P2 over P2, respectively whereas P1P2 and P2P1 represent the coating of P1 over P2 and vice versa. Fig. 1 shows the typical film structure prepared in this work. After this, these TiO_2 photoelectrodes were dried in the air at room temperature for 1 h followed by sintering at 500 °C for 30 min. An active area of 0.25 cm^2 was selected from sintered electrode and the electrodes were immersed in 3×10^{-4} M solution of N3 containing acetonitrile and tertiary butanol (in the volume ratio of 1:1) for 24 h.

In this work, the standard electrolyte was composed of 0.5 M LiI/0.05 M I_2 and 0.5 M TBP in acetonitrile. For compared the solvent effects, the electrolyte was only composed of 0.5 M lithium iodide/0.05 M iodine in different solvents. It is assumed that I^- and I_2 immediately formed I_3^- in this solution. The specified composition of the electrolyte solution was sprayed on both the dye-immobilized photoanode and Pt sputtered (thickness of Pt is 100 nm) FTO glass.

The DSSC cell was fabricated by keeping an ionomer resin (Surlyn 1702, Dupont, thickness of 60 μm) between the two electrodes and two holes were made on the resin. The whole set-up was heated at 90 °C on a hot plate till all the resin had been melted. After the cell was cooled at room temperature, the electrolyte was injected into the space between the electrodes through these two holes. Finally, these two holes were sealed completely by the Torr Seal® cement (Varian, MA, USA).

The TiO_2 film thickness was measured by using a profilometer (Sloan Dektak 3030). The TiO_2 surface area, pore diameter, pore volume, and particle diameter were measured by Brunauer–Emmett–Teller (BET) method, using Accelerated Surface Area and Porosimetry (Micrometrics Instruments ASAP 2010). The photoelectrochemical characterizations of the DSSCs were carried out by using an AM 1.5 simulated light radiation. The light source was a 450 W Xe lamp (#6266, Oriel) equipped with a water-based IR filter and AM 1.5 filter (#81075, Oriel). The photovoltage transients of assembled devices were recorded with a digital oscilloscope (LeCroy, model LT322). Pulsed laser excitation was applied by a frequency-doubled Q-switched Nd:YAG laser (Spectra-Physics laser, model Quanta-Ray GCR-3-10) with 2 Hz repetition rate at

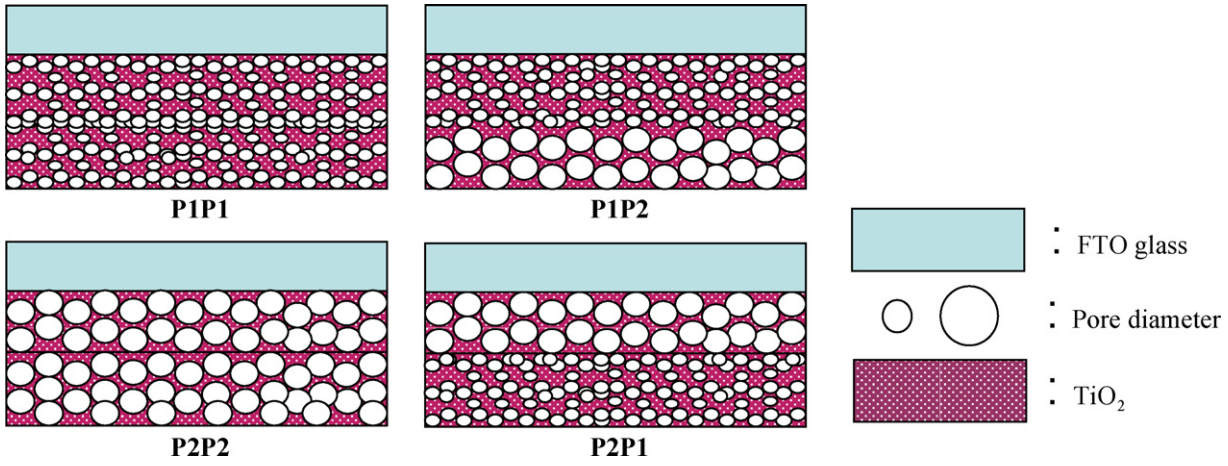

Fig. 1. Morphological structure of the different TiO_2 electrodes obtained by successive coating of P1 and P2 TiO_2 pastes on FTO substrate.

532 nm and 7 ns pulse width at half-height. The beam size was larger than 0.25 cm^2 to cover the area of the device with incident energy of 1 mJ cm^{-2}.

Photoelectrochemical characteristics and the ac-impedance measurements of the DSSCs were recorded with a potentiostat/galvanostat (PGSTAT 30, Autolab, Eco-Chemie, the Netherlands) under 100 mW cm^{-2}. EIS of DSSC was performed under constant light illumination and open-circuit conditions. The applied bias voltage and ac amplitude were set at open-circuit voltage of the DSSC and 10 mV between the FTO/Pt counter electrode and the FTO/TiO_2/dye working electrode, respectively [24]. Besides, the frequency range explored was 10 mHz to 65 kHz.

3. Results and discussion

3.1. The effect of TiO_2 morphology on the DSSCs

It is well known that the addition of PEG to the TiO_2 colloidal solution, after autoclaving, influences the porosity of the TiO_2 electrode [19]. The P1 and P2 which were prepared by the addition of 30 wt% (with respect to TiO_2) of PEG with the corresponding molecular weights of 20,000 and 200,000, respectively, and the surface structures are shown in Fig. 2. The coil size of a polymer is commonly represented by the radius of gyration (R_g), $R_g = C(M_w)^{1/2}$, where M_w (g mol^{-1}) is the molecular weight of the polymer and C is a constant depending on the properties of the solvent. It has been determined that C is 0.063 nm (g mol^{-1})$^{-1/2}$ for PEG in a good solvent [25]. It was expected that the TiO_2 pastes containing different molecular weight of PEG could result in the TiO_2 films have different distribution of pore diameters. It was found that the TiO_2 film prepared by P1 paste shows a smaller pore structure, and that

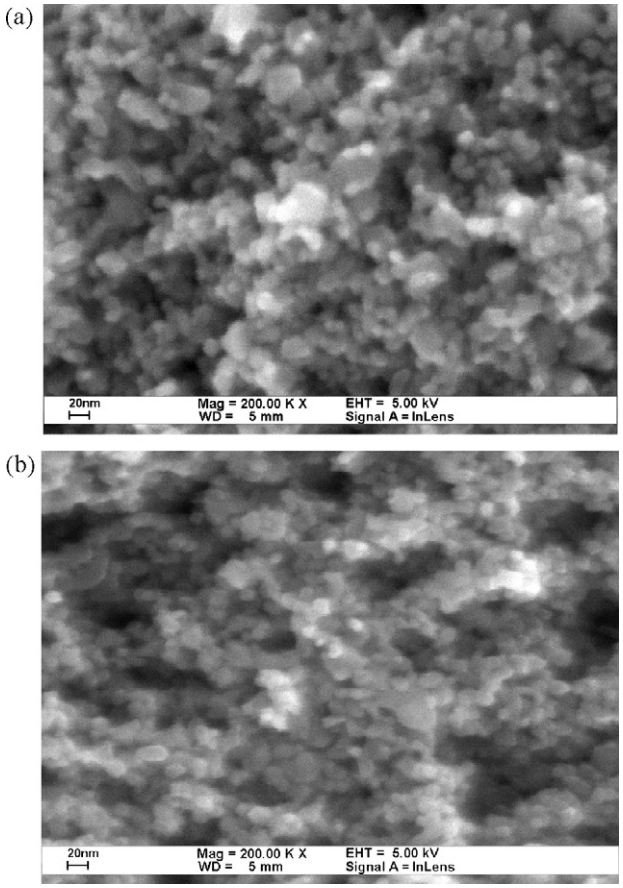

Fig. 2. The SEM images of the morphologies of P1 and P2 TiO_2 films.

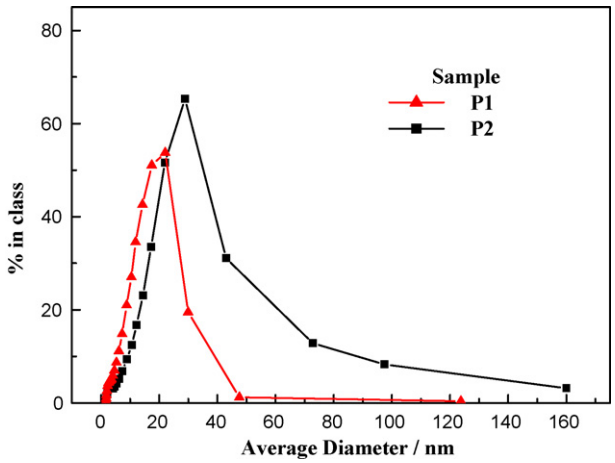

Fig. 3. Average pore diameters of P1 and P2 TiO_2 films obtained from BET measurement.

Table 1
The specific surface area, pore diameter, pore volume and average particle diameter of P1 and P2 TiO_2 photoelectrodes obtained from BET measurement and SEM micrograph.

Sample	Surface area (m^2 g^{-1})	Pore diameter (nm)	Pore volume (cm^3 g^{-1})	TiO_2 particle size[a] (nm)
P1	80.4	11.5	0.29	20
P2	67.1	18.9	0.38	

[a] The size of TiO_2 nanoparticle was measured by SEM.

prepared by P2 paste has a larger pore diameter. The penetration of electrolyte depended on the pore size of TiO_2 film. Therefore, the average pore diameters of P1 and P2 TiO_2 films determined from Brunauer–Emmett–Teller (BET) measurement are shown in Fig. 3 and listed in Table 1. The surface area and the pore diameter of P1 were found out to be 80.4 m^2 g^{-1} and 11.5 nm and P2 to be 67.1 m^2 g^{-1} and 18.9 nm, respectively. Further, the P1 TiO_2 electrode has smaller pore size than the P2 and the pore diameter distribution of P1 is also narrower than P2. We have investigated previously the influence of lifetime of the TiO_2 electrode as well as the performance of the DSSC by varying the amounts of PEG content in the TiO_2 electrode. The electron lifetime (τ_e) decreases and the value of the D_e increases with the increase in PEG content [26]. It is confirmed that the morphology of the TiO_2 electrodes greatly depends on the composition and the addition of the PEG.

The influences of these pore distribution patterns of the various TiO_2 films are also reflected on the absorption spectra taken for the above materials. From Fig. 4, it is understandable that the P1P1 TiO_2 electrode has highest absorption which follows P1P2, P2P1 and P2P2 and this trend was correlated with decrease in the surface area from P1P1 to P2P2.

Table 2 shows the comparative performances of DSSCs associated with the different TiO_2 electrodes under the identical thickness

Table 2
Photovoltaic parameters and electron lifetimes of DSSCs obtained with different TiO_2 morphologies. The thickness of the TiO_2 electrodes was 17.2 ± 0.5 μm.

Sample	τ_e (ms)[a]	R_{ct2} (Ω)[b]	$C_{\mu 2}$ (mF)[b]	J_{SC} (mA cm^{-2})	V_{OC} (V)	η (%)	FF
P1P1	1.40	49.49	4.50	16.84	0.72	7.63 ± 0.2	0.63
P1P2	1.43	59.86	4.24	15.53	0.71	6.84 ± 0.2	0.62
P2P1	2.25	39.51	3.82	17.64	0.74	8.35 ± 0.2	0.64
P2P2	2.20	50.86	2.61	16.40	0.74	7.76 ± 0.2	0.64

[a] The average electron lifetime (τ_e) obtained from transient photovoltage measurement.
[b] Obtained from EIS measurement.

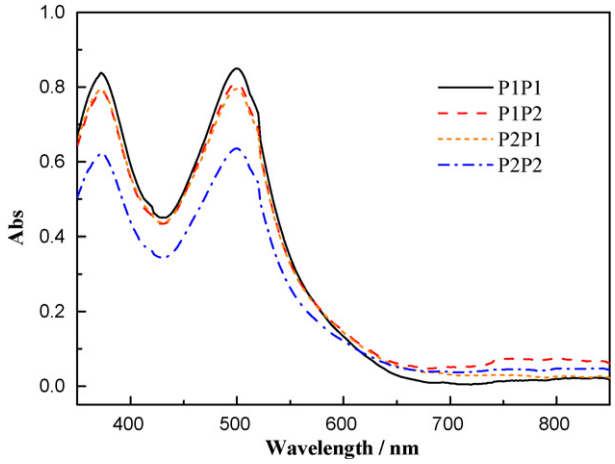

Fig. 4. Absorption spectra of various TiO_2 electrodes showing the influences of the pore distribution patterns.

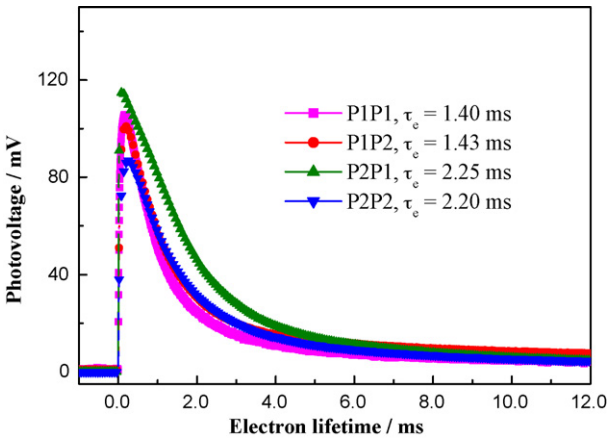

Fig. 6. Transient photovoltage measurements of various TiO_2 electrodes under identical conditions.

of 17.2 ± 0.5 μm. Among these different types of coated materials, P2P1 shows higher efficiency, which the short circuit current density (J_{SC}) is 17.64 mA cm^{-2} and the open circuit potential (V_{OC}) is 0.74 V with the cell conversion efficiency of 8.35%, than all the other TiO_2 electrode conformations. The reason for this behavior is due to the presence of large pores in the electrode materials coated with P2 which may allow the diffusion of more redox species inside the pores leading to high the electron lifetime in TiO_2 electrode (see latter).

EIS analysis could help to understand the electrode kinetics of the DSSCs by analyzing the variations in impedances associated with the different configurations of applied cells [12–15]. Fig. 5a and b shows the equivalent circuit and the typical Nyquist plot of the DSSCs having the four types of the TiO_2 film, respectively. Three semicircles were observed clearly in the measured frequency range of 10 mHz–65 kHz. The ohmic serial resistance (R_S) in the high-frequency region corresponds to the electrolyte and the FTO resistance, while the resistances R_{ct1}, R_{ct2} and R_{diff} relate to charge-transfer processes occurring at the Pt counter electrode in the high frequency region, resistance for TiO_2/electrolyte interface and Nernstian diffusion within the electrolyte in the low frequency region, respectively [27,28]. If we compare the impedance spectra of these four TiO_2 materials, the value of R_{ct2} of P2P1 was about 39.5 Ω which smaller than that of others (Fig. 5a). This proves that though the surface area of P2P1 electrode is smaller than that of P1P1 electrode, adequate pore sizes are available in the case of P2P1 for the facile transport of the redox couple in the TiO_2 interface thereby reducing the corresponding resistance at the interface [29]. From the Bode phase plot as shown in Fig. 5b, the characteristic frequency peak based on P2P1 electrode shifted to lower frequency, indicating has a longer electron lifetime in P2P1 TiO_2 electrode.

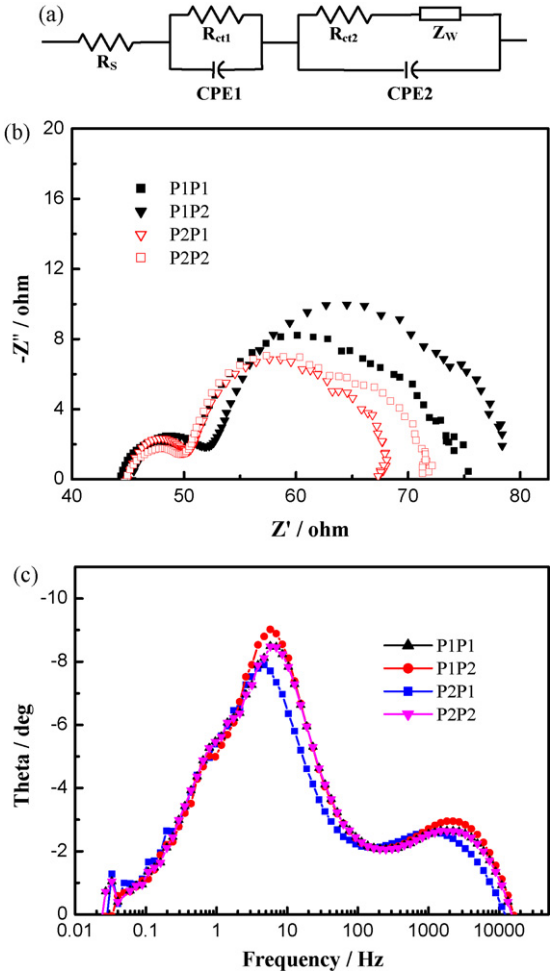

Fig. 5. (a) Equivalent circuit of the DSSC used in this study, (b) Nyquest plots and (c) Bode phase plots of the DSSCs based on various TiO_2 electrode materials.

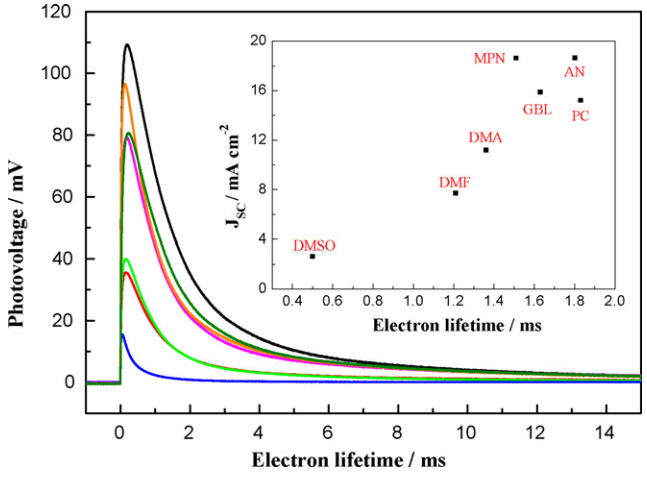

Fig. 7. Transient photovoltage measurements of P2P1 TiO_2 electrode in different solvents under identical condition. The inset shows the dependence of the J_{SC} of the DSSC on electron lifetime of the TiO_2 electrode in different solvents.

Furthermore, the laser-induced photovoltage transient studies on the effect of different TiO_2 morphologies are shown in Fig. 6. It is found that the electron lifetimes based on P2P1 and P2P2 were similar (ca. 2.2 ms) and had longer electron lifetime than P1P1 and P1P2 (ca. 1.4 ms, shown in Table 1). This supported the above results measured by EIS and indicated that the first coating of TiO_2 film effectively decides the adhesion between FTO and TiO_2 film, and the electron lifetime in the TiO_2 electrodes.

From our earlier works [19], it was observed that that the cell fabricated with the TiO_2 electrode having small diameter of the TiO_2 particles and larger pore size would have better electron transport property. Therefore, the coating of P2 on FTO can facilitate the electron transport property and reduce diffusion resistance of the inner TiO_2 electrode. This could explain why the P2P1 TiO_2 electrode with the optimum thickness exhibits the lowest R_{ct2} and the best performance in this study.

3.2. The solvent effect on the DSSCs

The effect of different solvents on the photovoltaic performance of the DSSC containing P2P1 TiO_2 electrodes was studied. Table 2 shows the cell performances of the DSSCs based on different solvents. From this table, it is noted that the DSSC containing acetonitrile (AN) has highest efficiency and the efficiencies of the DSSCs with different solvents are arranged in the following order: AN > MPN > PC > GBL > DMA > DMF > DMSO. Surprisingly, in the case of DMF and DMSO, the total performance was very low though the open circuit voltages (V_{OC}) were significantly higher than others.

The above results are also reflected on the laser-induced transients measurements of electrons in the TiO_2 electrodes with different solvents. Fig. 7 shows such measurements for different solvents and the inset shows the dependence of the J_{SC} of the DSSC with various solvents against their respective electron lifetimes in

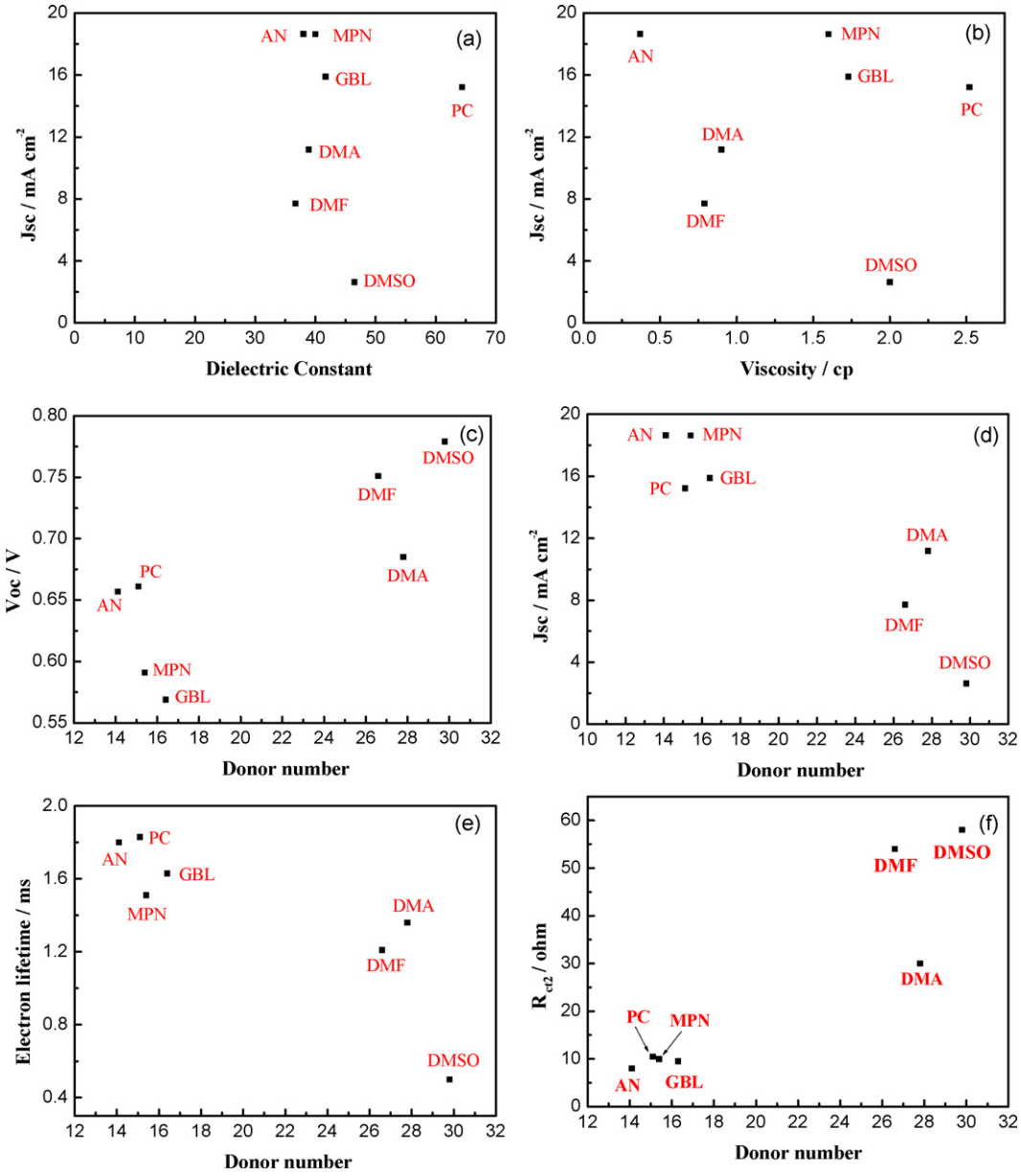

Fig. 8. (a) and (b) show the dependence of J_{SC} of the DSSC on dielectric constant and viscosity of different solvents, respectively; (c), (d), and (f) show the dependence of the donor number of different solvents against the V_{OC}, J_{SC} and R_{ct2} of the DSSCs. (e) shows the relationship between the donor number of solvents and the electron lifetimes in TiO_2 electrode in respective solvents.

Table 3
Photovoltaic parameters and electron lifetimes of DSSCs obtained with different solvents.

Solvent[a]	ξ (cp)[b]	DN[c]	J_{SC} (mA cm^{-2})	V_{OC} (V)	η (%)	FF
AN	0.37	14.1	18.62	0.657	7.73	0.632
MPN	1.60	15.4	18.63	0.591	7.01	0.637
PC	2.52	15.1	15.21	0.661	6.29	0.626
GBL	1.73	18.0	15.89	0.569	5.30	0.587
DMA	0.90	27.8	11.18	0.685	4.90	0.640
DMF	0.79	26.6	7.71	0.751	4.22	0.730
DMSO	2.00	29.8	3.82	0.779	2.06	0.692

[a] Only added LiI (0.5 M)/I_2 (0.05 M) in solvent.
[b] Viscosity of solvent at 25 °C.
[c] Donor number of solvent.

the TiO_2 electrode. In this, the electron lifetimes on the TiO_2 electrodes in different solvents correlate well with the J_{SC} of the DSSCs with these solvents and this follows our earlier experimental results obtained on the performances of the DSSCs with different solvents.

The photoelectrochemical properties of the DSSCs with various solvents have been related with their physical properties (Table 3). For example, Fig. 8a and b shows the dependence of the J_{SC} of the DSSCs with above solvents toward their dielectric constant and viscosity. It is found that those two physical properties do not show any specific correlation with the J_{SC} of the DSSCs. On the other hand, donor numbers of solvents reveal better relationship with the V_{OC} (Fig. 8c), J_{SC} (Fig. 8d), R_{ct2} (Fig. 8f, obtained from the EIS studies) of the DSSCs and the electron lifetimes in the TiO_2 electrode containing the above solvents (Fig. 8e). The V_{OC} and R_{ct2} increase with increasing of donor number while the J_{SC} and τ_e have a totally reverse change tendency, which has a similar trend as the reported results by Fukui et al. [21]. From the above studies, it is observed that the higher donor number of the solvents, the lower will be the performances of the DSSCs.

The donor–acceptor reaction between the non-aqueous solvents and iodine was investigated by Kebede and Lindquist [14]. It is revealed that the donor number of solvent is important in solvents interaction with iodine and that can control the equilibrium of iodine (I^-) and tri-iodide (I_3^-) ions in solvents. With the increase of donor number of solvent, the free I_3^- concentration decrease and free I^- concentration increase, which improved the hole collection by I^- [30]. The increase of V_{OC} can be explained according to the following equation [31,32]:

$$V_{oc} = \left[\frac{kT}{e}\right] \ln\left(\frac{I_{inj}}{n_{cb}k_{et}\left[I_3^-\right]}\right) \quad (1)$$

where k is Boltzmann constant, T is the absolute temperature, e is the electronic elementary charge, I_{inj} is the flux of charge resulting from sensitized injection, n_{cb} is the concentration of electrons at the TiO_2 surface, k_{et} is the reaction rate constant of I_3^- dark reaction on TiO_2 surface, and the $[I_3^-]$ is the concentration of I_3^- in electrolyte. Solvents with higher donor number make for easier formation of complex between solvents and iodine, resulting in the V_{OC} increase with increasing donor number of solvents. In addition, the solvents with higher donor number are more Lewis basicity and easier reacting with the bare Lewis acidic TiO_2 surface which shows higher efficient for blocking the active sites of TiO_2 electrode and decreasing the rate of I_3^- reduction (k_{et}), so that increases the V_{OC}. Alternatively, as the Lewis basic characteristic of additive in electrolyte, e.g. TBP, the higher donor number solvents absorb on TiO_2 surface may negative shift the flat band potential (V_{FB}) of TiO_2 electrode [33], which decreases the driving force for excited dye to inject electrons into the conduction band edge of TiO_2 and leads to the decrease of J_{SC} and increase of V_{OC}.

Moreover, they also have low electron lifetimes in the TiO_2 electrodes and as a result of this, the R_{ct2} of the DSSC will be very high. The reason for this anomalous behavior may be correlated with the presence of solvent–dye interaction on the surface of the TiO_2 photoelectrode. In order to characterize such interaction, dye immobilized TiO_2 electrodes were washed repeatedly with AN till the excess dye had been removed and each electrode was dipped separately in 5 ml of the solvents for 1 h and the absorption spectra of these solvents were recorded immediately (Fig. 9). Surprisingly, UV–vis spectra taken for these solvents showed absorption characteristics for the N3 dye molecules, which revealed that the solvent molecules desorbed the N3 dye molecule from the surface of the TiO_2 to some extent. From the intensity of the absorption spectra, it is understandable that the characteristics of desorption follow the order DMSO > DMF > DMA. Further, in the Bode plot (Fig. 10), it is found that when the DMSO, DMF and DMA were used as the electrolyte solvents, the characteristic frequency peaks of TiO_2 obviously shifted to higher frequency than that of AN. The characteristic frequency can be related to as the inverse of the recombination lifetime (τ_r) [34]. This behavior is due to the dye desorption and decrease in electron lifetime. Those results indicated that both the donor number and desorption properties of the solvents play an important role in tuning the performance of the DSSCs.

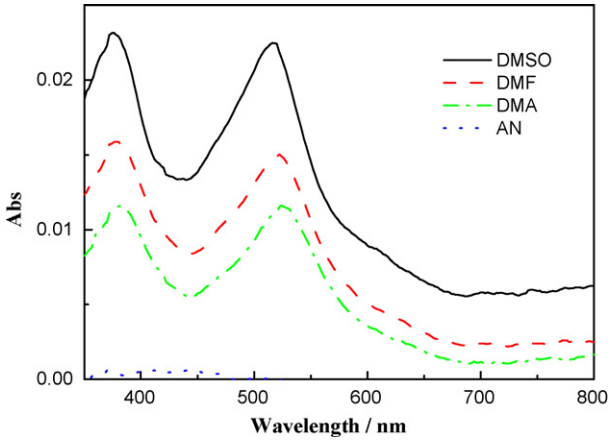

Fig. 9. The absorption spectra based on DMSO, DMF and DMA, respectively, indicating the dye desorption from the TiO_2 photoelectrode.

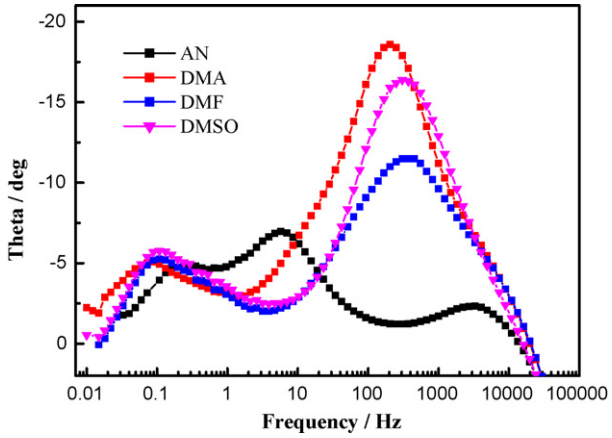

Fig. 10. The Bode phase plots of the DSSCs based on AN, DMA, DMF and DMSO solvents, respectively.

4. Conclusion

The effects of different TiO_2 surface morphology and solvents on the solar cell performance of the DSSC were investigated in this work. From these investigations, it is observed that the

TiO_2 film morphology strongly influences the performance of the DSSC. Among the DSSC having four different TiO_2 surface morphology, P2P1 TiO_2 electrode showed highest performance and this may be related with their better electron transport and less ion diffusion resistance than the other electrodes. EIS and electron lifetime measurements also confirm this. The DSSC performance depends strongly on the nature of the solvent. The performance order for the DSSCs containing different solvents were AN > MPN > PC > GBL > DMA > DMF > DMSO. Better correlation was found out from the donor number rather than the dielectric constant and viscosity of different solvents. The electron lifetime measurement of TiO_2 electrodes in different solvents also follows this. Furthermore, solvents such as DMA, DMF and DMSO desorbs the dye molecules from the TiO_2 electrode as noted from the absorption spectra and this may also decrease the performance of the DSSC.

Acknowledgements

This work was financially supported by the Academia Sinica, Taipei, Taiwan, the Republic of China, under grant AS-97-TP-A08. We also want to thank Professor King-Chuen Lin and his research group members, of Department of Chemistry, National Taiwan University, for the help in making the pulsed laser apparatus available to us.

References

[1] M. Grätzel, J. Photochem. Photobiol. A: Chem. 164 (2004) 3.
[2] B. O'Regan, M. Grätzel, Nature 353 (1991) 737.
[3] S. Kambe, K. Murakoshi, T. Kitamura, Y. Wada, S. Yanagida, H. Kominami, Y. Kera, Sol. Energy Mater. Sol. Cells 61 (2000) 427.
[4] C.J. Barbe', F. Arendse, P. Comte, M. Jirousek, F. Lenzmann, V. Shklover, M. Grätzel, J. Am. Ceram. Soc. 80 (1997) 3157.
[5] A. Kay, M. Grätzel, Chem. Mater. 14 (2002) 2930.
[6] Z.S. Wang, C.H. Huang, Y.Y. Haung, Y.J. Hou, P.H. Xie, B.W. Zhang, H.M. Cheng, Chem. Mater. 13 (2001) 678.
[7] Z.-S. Wang, H. Kawauchi, T. Kashima, H. Arakawa, Coord. Chem. Rev. 248 (2004) 1381.
[8] M.K. Nazeeruddin, A. Kay, I. Rodicio, R. Humphry-Baker, E. Muller, P. Liska, N. Vlachopoulos, M. Grätzel, J. Am. Chem. Soc. 115 (1993) 6382.
[9] M.K. Nazeeruddin, P. Pechy, T. Renouard, S.M. Zakeeruddin, R. Humphry-Baker, P. Comte, P. Liska, C. Le, E. Costa, V. Shklover, L. Spiccia, G.B. Deacon, C.A. Bignozzi, M. Grätzel, J. Am. Chem. Soc. 123 (2001) 1613.
[10] T. Renouard, R.-A. Fallahpour, M.K. Nazeeruddin, R. Humphry-Baker, S.I. Gorelsky, A.B.P. Lever, M. Grätzel, Inorg. Chem. 41 (2002) 367.
[11] S.M. Zakeeruddin, M.K. Nazeeruddin, P. Pechy, F.P. Rotzinger, R. Humphry-Baker, K. Kalyanasundaram, M. Grätzel, V. Shklover, T. Haibach, Inorg. Chem. 36 (1997) 5937.
[12] P. Wang, S.M. Zakeeruddin, J.E. Moser, R. Humphry-Baker, P. Comte, V. Aranyos, A. Hagfeldt, M.K. Nazeeruddin, M. Grätzel, Adv. Mater. 16 (2004) 1806.
[13] Y. Saito, W. Kubo, T. Kitamura, Y. Wada, S. Yanagida, J. Photochem. Photobiol. A: Chem. 164 (2004) 153.
[14] Z. Kebede, S.-E. Lindquist, Sol. Energy Mater. Sol. Cells 57 (1999) 259.
[15] K. Hara, T. Horiguchi, T. Kinoshita, K. Sayama, H. Arakawa, Sol. Energy Mater. Sol. Cells 70 (2001) 151.
[16] F. Cecchet, A.M. Gioacchini, M. Marcaccio, F. Paollucci, S. Roffia, M. Alebbi, C.A. Bignozzi, J. Phys. Chem. B 106 (2002) 3926.
[17] E. Olsen, G. Hagen, S.E. Lindquis, Sol. Energy Mater. Sol. Cells 63 (2000) 267.
[18] N. Papageorgiou, W.F. Maier, M. Grätzel, J. Electrochem. Soc. 144 (1997) 876.
[19] K.M. Lee, V. Suryanarayanan, K.C. Ho, Solar Energy Mater. Solar Cells 90 (2006) 2396.
[20] Q. Shen, T. Toyoda, Thin Solid Films 438–439 (2003) 167.
[21] A. Fukui, R. Komiya, R. Yamanaka, A. Islam, L. Han, Solar Energy Mater. Solar Cells 90 (2006) 649.
[22] S. Kambe, S. Nakade, T. Kitamura, Y. Wada, S. Yanagida, J. Phys. Chem. B 106 (2002 2967).
[23] S.A. Haque, Y. Tachibana, R.L. Willis, J.E. Moser, M. Grätzel, D.R. Klug, J.R. Durrant, J. Phys. Chem. B 104 (2000) 538.
[24] J. van de Lagemaat, N.G. Park, A.J. Fra, J. Phys. Chem. B 104 (2000 2044).
[25] C. Vandermiers, P. Damman, M. Dosiere, Polymer 39 (1998) 5627.
[26] K.M. Lee, V. Suryanarayanan, K.C. Ho, Solar Energy Mater. Solar Cells 91 (2007) 1416.
[27] K. Kalyanasundaram, M. Grätzel, Coord. Chem. Rev. 77 (1998) 347.
[28] A. Fillinger, D. Soltz, B.A. Parkinson, J. Electrochem. Soc. 149 (2002) A1146.
[29] E. Hawlicka, R. Grabowski, B. Bunsenges, Phys. Chem. 94 (1990) 158.
[30] D. Cahen, G. Hodes, M. Grätzel, J.F. Guillemoles, I. Riess, J. Phys. Chem. B 104 (2000 2053).
[31] S.Y. Huang, G. Schlichthorl, A.J. Nozik, M. Grätzel, A.J. Frank, J. Phys. Chem. B 101 (1997) 2576.
[32] H. Greijer, J. Lindgren, A. Hagfeldt, J. Phys. Chem. B 105 (2001) 6314.
[33] T.S. Kang, K.H. Chun, J.S. Hong, S.H. Moon, K.J. Kim, J. Electrochem. Soc. 147 (2000) 3049.
[34] G. Schlichthorl, S.Y. Huang, J. Sprague, A.J. Frank, J. Phys. Chem. B 101 (1997) 8141.